Multifrequency tomographic reconstruction in terahertz imaging

Ke Chen and David Castañón ECE Department, Boston University

Motivation

Much of the recent interest in terahertz (THz) imaging stems from its ability to reveal unique spectral characteristics of chemicals in THz range and thus to fingerprint explosives. Short-pulse THz sources provide broadband excitation, but most inversion techniques as diffraction tomography work construct images for single frequencies. In this work, we explore alternatives for joint image formation using multiple frequencies for enhanced explosives detection.

Background

I. Modality: transmission tomography

Object field: $o(\boldsymbol{r}, f) = \tilde{n}(\boldsymbol{r}, f)^2 - 1$
Measurements: $u_s(\boldsymbol{r}) = u(\boldsymbol{r}) - u_0(\boldsymbol{r})$

- Scattered field in the form of Green's function

$$u_s(\boldsymbol{r}) = -k_0^2 \int g(\boldsymbol{r} - \boldsymbol{r}')o(\boldsymbol{r}')u(\boldsymbol{r}')\, d\boldsymbol{r}'$$

- Written in Fourier transform terms under the first Born Approximation $u(\boldsymbol{r}) \approx u_0(\boldsymbol{r})$

$$U_s(\boldsymbol{\omega}) = G(\boldsymbol{\omega})\{O(\boldsymbol{\omega}) * U_0(\boldsymbol{\omega})\} = G(\boldsymbol{\omega})2\pi O(\boldsymbol{\omega} - \boldsymbol{k})$$

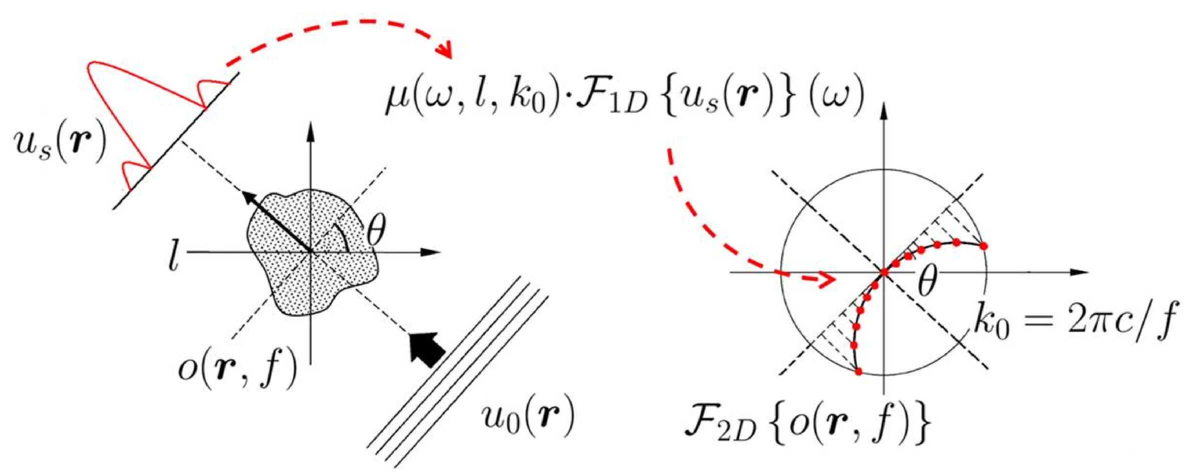

Fourier Diffraction Theorem relates scattering with object spectrum

- Problem formulation for tomographic imaging based on Fourier Diffraction Theorem[1]

$$\boldsymbol{y} = \boldsymbol{\Psi}\boldsymbol{x}$$

$\boldsymbol{x} \in \mathbb{C}^{N^2}$ object field of interest
$\boldsymbol{y} \in \mathbb{C}^{K}$ Fourier transform of measured scattered data
$\boldsymbol{\Psi}$ nonuniform Fourier transform(NUFT) operator

II. Nonuniform FFT

$\mathcal{T}$: Fast approximation for the NUFT[2]

step 1. Point-wise scaling

step 2. Oversampled FFT

step 3. Min-max optimized Kaiser-Bessel interpolation using small local neighborhoods

Methods

I. Reconstruct frequency by frequency

Reconstruct object field $\boldsymbol{x}_m \in \mathbb{C}^{N^2}$ and boundary field $\boldsymbol{s}_m \in \mathbb{R}^{N^2}$ at each frequency $f_m, m = 1 \ldots M$:

$$\|\boldsymbol{y}_m - \mathcal{T}_m\boldsymbol{x}_m\|^2 + \alpha^2\|\mathcal{D}\boldsymbol{x}_m\|^2_{W_s} + \beta^2\|\mathcal{D}\boldsymbol{s}_m\|^2 + \frac{1}{\beta^2}\|\boldsymbol{s}_m\|^2$$

- Data-fidelity term in *frequency* domain
- Smoothness penalty term in *spatial* domain, where $\mathcal{D}$ is a derivative operator
- Spatially varying weighting: $W_s = \mathrm{diag}[(1 - [\boldsymbol{s}_m]_i)^2]$
- Alternating coordinate minimization
- Speed up with $\mathcal{T}_m \approx \boldsymbol{\Psi}_m$

II. Joint multifrequency and spatial prior

- Boundary field $\boldsymbol{s}$ is *invariant* across frequencies
- Joint multifrequency to reconstruct $(\underline{\boldsymbol{x}}, \boldsymbol{s})$[3]: $\underline{\boldsymbol{x}} = [\boldsymbol{x}_1, \ldots, \boldsymbol{x}_M]^T$

$$\|\underline{\boldsymbol{y}} - \mathcal{T}\underline{\boldsymbol{x}}\|^2 + \alpha^2\|\tilde{\mathcal{D}}\underline{\boldsymbol{x}}\|^2_{\tilde{W}_s} + \beta^2\|\mathcal{D}\boldsymbol{s}\|^2 + \frac{1}{\beta^2}\|\boldsymbol{s}\|^2$$

where $\mathcal{T} = \mathrm{diag}[\mathcal{T}_m]$, matrix with $\sim$ stands for kronecker product of this matrix with $\mathbf{I}$, $\dim(\mathbf{I}) = M$

III. Combine spectral priors

- Known J components with spectral prior $\mathcal{E} \in \mathbb{C}^{M\times J}$

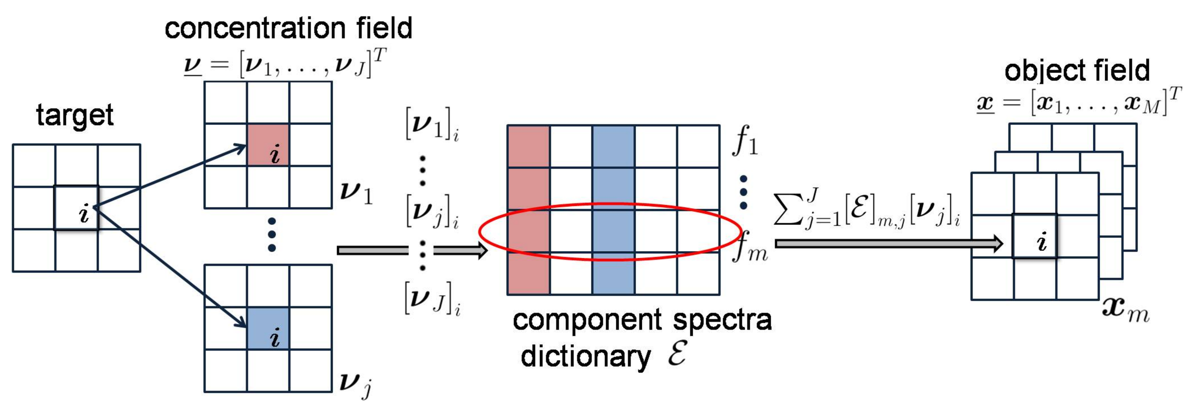

Relation between component concentration fields and object fields

- Linear transform $\mathcal{H}$[4]: $\underline{\boldsymbol{x}} = \mathcal{H}\,\underline{\boldsymbol{\nu}}$
- Joint multifrequency to reconstruct $(\underline{\boldsymbol{\nu}}, \boldsymbol{s})$: $\underline{\boldsymbol{\nu}} = [\boldsymbol{\nu}_1, \ldots, \boldsymbol{\nu}_J]^T : \boldsymbol{\nu}_j \in \mathbb{R}^{N^2},\ 0 \le [\boldsymbol{\nu}_j]_i \le 1$

$$\|\underline{\boldsymbol{y}} - \mathcal{T}\mathcal{H}\,\underline{\boldsymbol{\nu}}\|^2 + \alpha^2\|\tilde{\mathcal{D}}\underline{\boldsymbol{\nu}}\|^2_{\tilde{W}_s} + \beta^2\|\mathcal{D}\boldsymbol{s}\|^2 + \frac{1}{\beta^2}\|\boldsymbol{s}\|^2$$

where matrix with $\sim$ stands for kronecker product of this matrix with $\mathbf{I}$, $\dim(\mathbf{I}) = J$

Results

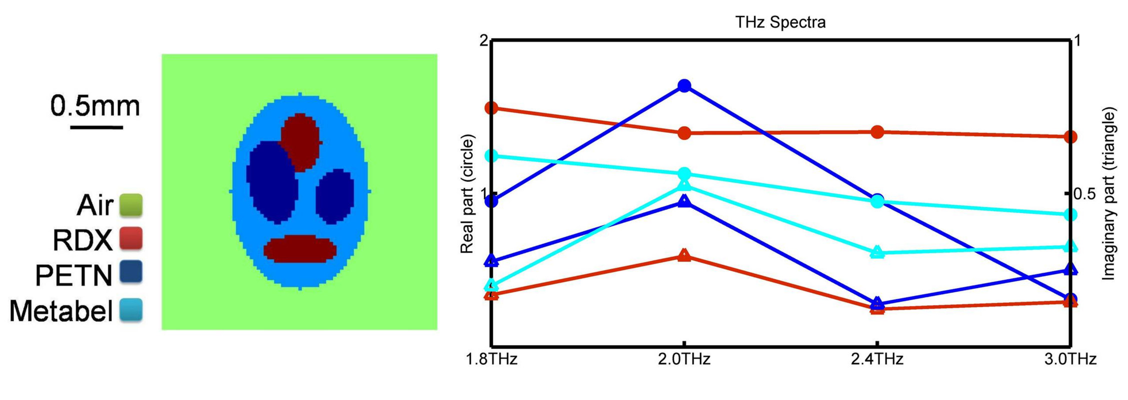

Phantom and explosives spectral priors

An 81 × 81 phantom consisting of 3 explosives and air as background was generated with spectral prior given in [5][6]. We simulated THz incident fields at 19 projection angles, and collected complex amplitude of the scattering at 4 frequencies for reconstruction.
Each method was evaluated under various levels of Gaussian noise. Every pixel in the reconstructed fields was classified using rule as follows: For Methods I and II, the class is chosen to minimize the Euclidean distance from the reconstructed susceptibilities at different frequencies to the spectral priors of the different explosives. For Method III, the most likely component is assigned to that pixel.

I. Reconstructions

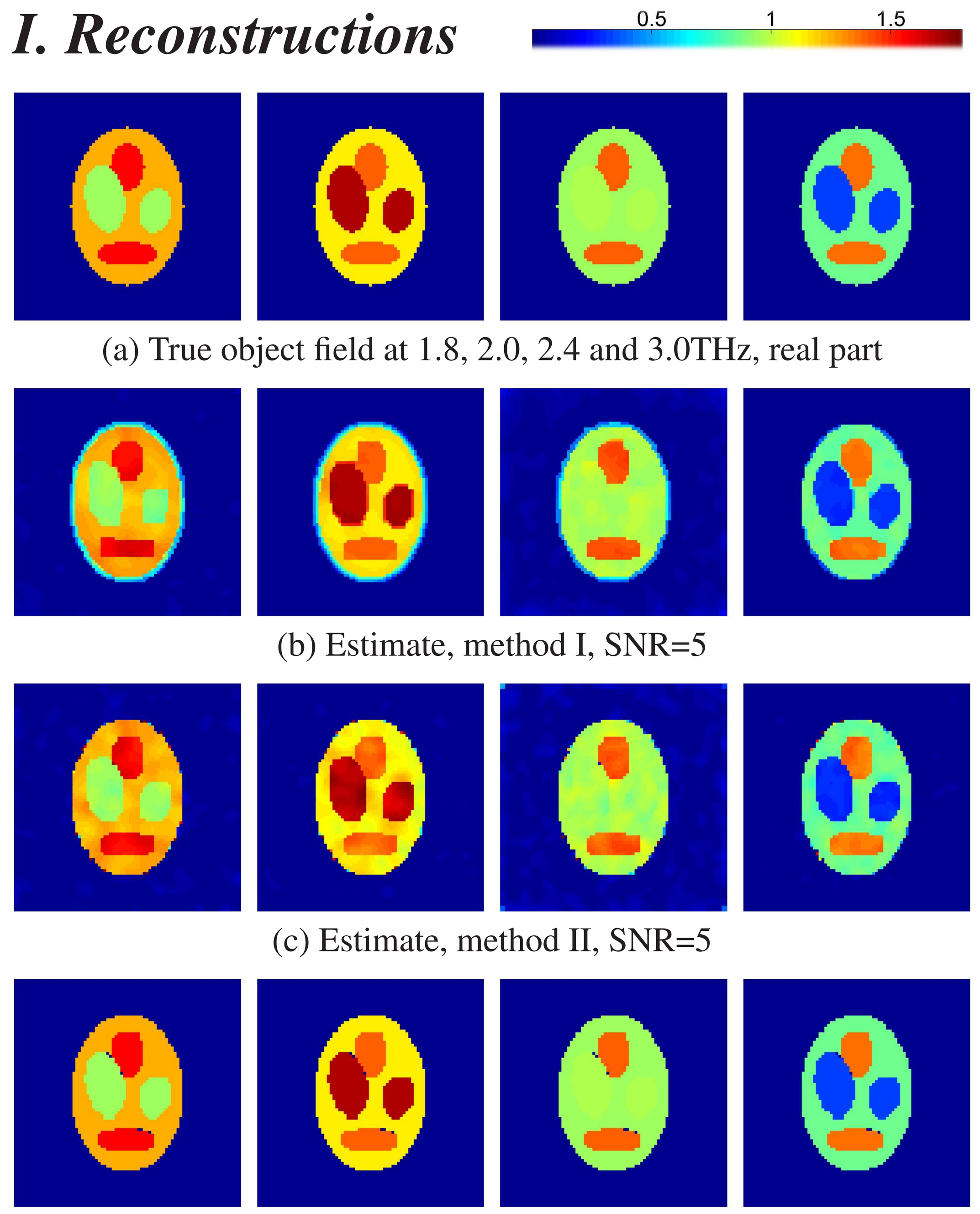

(a) True object field at 1.8, 2.0, 2.4 and 3.0THz, real part

(b) Estimate, method I, SNR=5

(c) Estimate, method II, SNR=5

(d) Estimate, method III, SNR=5

II. Performance comparisons

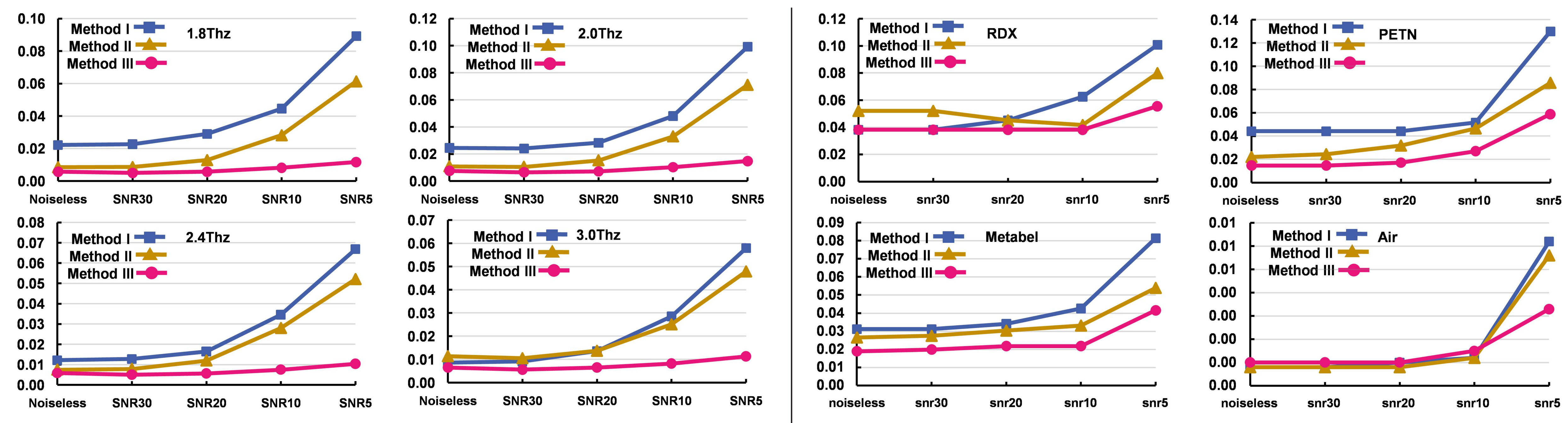

Average absolute error in object field reconstruction

Recognition error rate $\left(\frac{\text{\# false positive + \# false negative}}{\text{\# pixels in ground truth}}\right)$

Spatial information may not be well extracted at certain frequencies in Method I due to factors such as lower resolution (i.e. longer wavelength) and feature ambiguity. Method II, the joint multifrequency approach, improves the estimation of the boundary field and thus enhances the accuracy of the reconstruction and the subsequent recognition. Method III achieves better reconstruction and recognition by imposing spectral prior into the inverse process and consequently forcing spatial consistency during the reconstruction.

References

[1] A. Kak, M. Slaney, *Principles of Computerized Tomographic Imaging*, 2001.
[2] J. Fessler, B. Sutton, *IEEE Tr. Sig. Proc.* vol. 51, no. 2, pp. 560-574, 2003.
[3] R. Weisenseel, Ph.D. diss., Boston University, 2004.
[4] A. Li and et al. *Appl. Opt.* vol. 44, no. 10, pp.1948-1956, 2005.
[5] J. Chen and et al. *Opt. Express* vol. 15, no. 19, 2007.
[6] C. Baker and et al. *Proc. of IEEE* vol.95, no. 8, pp1559-1565, 2007.

Acknowledgement

This work was supported by Gordon-CenSSIS (award number EEC-9986821) and the U.S. Department of Homeland Security (award number 2008-ST-061-ED0001). The views and conclusions contained in this document are those of the authors and should not be interpreted as necessarily representing the official policies, either expressed or implied of the U.S. Department of Homeland Security.

Relationship to CenSSIS and ALERT